ISBN: 978-3-95450-231-8 ISSN: 2673-5490 doi: 10.18429/JACoW-IPAC2023-THPM095

FINITE ELEMENT STUDY OF AC LOSSES IN THE SUPERCONDUCTING COIL OF THE NHa C400 CYCLOTRON

L. Denis*, C. Geuzaine, B. Vanderheyden, University of Liège, Liège, Belgium
W. Kleeven, V. Nuttens, Ion Beam Applications, Louvain-la-neuve, Belgium
P. Velten, Normandy Hadrontherapy, Caen, France

Abstract

The NHa C400 is the first compact superconducting cyclotron used for carbon therapy in the world. Carbon therapy is particularly effective for treating radiation-resistant tumors, as compared to more conventional radiotherapy techniques. In this work, a 3D finite element model of the Nb-Ti coil has been developed using the open-source solver GetDP. First, an accurate representation of the DC magnetic fields, required for beam dynamics computation, is obtained. Second, analytical models of increasing complexity for hysteresis losses in the superconducting filaments are investigated. For discussing their accuracy, a single filament model has been developed. Third, the heat loss in the Nb-Ti coils during energization of the cyclotron is evaluated based on a multi-scale approach involving the single filament model.

INTRODUCTION

The C400 cyclotron for hadron therapy is the result of the cooperation between Ion Beam Applications (IBA) and Normandy Hadrontherapy (NHa). In order to characterize the thermal behavior of the coil during its energization ramp, a framework for the numerical evaluation of AC losses in superconducting coils is proposed. First, analytical predictions for losses are presented. A numerical model at the scale of a single filament, using the GetDP finite-element software [1], is investigated to assess their accuracy and their range of validity. Based on the results obtained, total losses during the C400 ramp-up are computed using a multi-scale approach.

MAGNETIC CIRCUIT

The C400 cyclotron is an isochronous cyclotron with spiralized poles and an elliptical gap [2]. As this study focuses on the superconducting coil, the geometry of the magnet has been simplified to a four-fold rotational symmetry with a reflection plane in the middle of the pole gap. The modified vector potential a^*-formulation is chosen to deal with the non-linear behaviour of the ferromagnetic yoke. It is described in [3]. The flux density computed in the median plane of the cyclotron at nominal current is shown in Fig. 1. The peak field on the conductor is 3.68 T.

The C400 coil conductor is based on wire-in-channel technology, in which the composite copper-Nb-Ti (Nb-Ti filaments of diameter $d_f = 51$ µm) wire is embedded inside a copper channel. The coil is cooled down by a liquid helium bath at $T_{\mathrm{He}} = 4.2$ K.

* lsdns21@gmail.com

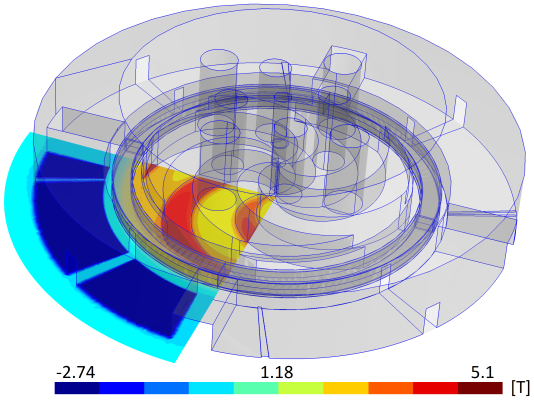

Figure 1: Upper magnetic circuit of the C400 used in this study and the median plane normal magnetic flux density b. For scale, the outer radius of the cyclotron is 3.34 m.

The main loss mechanisms inside the conductor are inter-filament coupling losses and hysteresis losses.

INTER-FILAMENT COUPLING LOSSES

The physical origin of the coupling losses in the copper matrix is the variation of the magnetic flux over several filaments inducing eddy currents between filaments. Assuming screening currents do not prevent the field from entering the composite, Carr [4] has developed an analytical expression for coupling losses q_c [W/m^3], assuming round composites of negligible diameter with respect to the pitch length:

$$q_c = \frac{\lambda}{\lambda_{st}} \frac{1}{\rho_{et}} \left(\frac{p}{2\pi} \right)^2 \left\| \frac{db}{dt} \right\|^2, \quad \rho_{et} = \rho_{Cu} \frac{1 + \lambda_{st}}{1 - \lambda_{st}}, \qquad (1)$$

with p [m] the filament twist pitch length, ρ_{et} [m] the effective transverse resistivity of the matrix, ρ_{Cu} [m] the electric resistivity of copper, $\lambda = 0.03$ the total Nb-Ti filling factor and $\lambda_{st} = 0.42$ the local Nb-Ti filling factor of the strand. At cryogenic temperature, magnetoresistance must be taken into account, as shown in [5] (p. 8-23).

HYSTERESIS LOSSES

State of the Art

Hysteresis losses occur inside Nb-Ti filaments immersed in a changing magnetic field. Carr [4] and Wilson [6] have derived analytical predictions for hysteresis losses per cycle in single filaments, using Bean's Critical State Model (CSM) [7]. The results are here adapted for computing the

ISBN: 978-3-95450-231-8 ISSN: 2673-5490 doi: 10.18429/JACoW-IPAC2023-THPM095

instantaneous power loss per unit volume $q_{\mathrm{hys},1}$ [W/m^3] during current ramp-up.

The transverse field loss per filament, assuming no transport current, an external uniform flux density of amplitude b_a and no critical current density dependence on field amplitude $\partial j_c/\partial b = 0$, can be obtained [4] as

$$q_{\mathrm{hys},1} = \frac{2}{3\pi} j_c d_f \dot{b}_a, \tag{2}$$

assuming full penetration ($b_a > b_p$) of the filament. The full penetration flux density is denoted $b_p = \mu_0\, j_c\, d_f/\pi$ with $\mu_0 = 4\pi 10^{-7}$ H/m. In the weak penetration regime, an adaptation of Carr's developments in a monotonic field ramp-up leads to

$$q_{\mathrm{hys},1} = \frac{64}{3\pi j_c \mu_0^2 d_f}\, b_a^2\, \dot{b}_a, \tag{3}$$

which should be valid in low field. Combining [4] the two regimes:

$$q_{\mathrm{hys},1} = \frac{1}{3\pi}\, \frac{2 j_c d_f b_a^2}{j_c^2 d_f^2 \mu_0^2/32 + b_a^2} \dot{b}_a. \tag{4}$$

The hysteresis losses at macroscopic scale are computed as $q_{\mathrm{hys}} = \lambda q_{\mathrm{hys},1}$.

Numerical Model

The accuracy of analytical approximations (Eq. (2), Eq. (3) and Eq. (4)) for transverse field losses is assessed with a finite element model of one single Nb-Ti filament.

Neglecting variations along the filament axis, only its circular cross-section is modeled in two dimensions. The diameter of the filament is $d_f = 51\,\mu$m. The outer domain, assumed non-conductive, is large and its diameter is $d_a = 500\,\mu$m. It has been chosen as non-conductive in order to assess the losses in the Nb-Ti only and to compare them with the CSM predictions.

The physics of Nb-Ti, assumed in the mixed state, is modeled through the power law [8,9] linking the current density j [A/m^2] to the electric field e [V/m]:

$$j = \frac{j_c}{e_c} \left(\frac{\|e\|}{e_c} \right)^{(1-n)/n} e, \tag{5}$$

with $e_c = 10^{-4}$ V/m by convention. The exponent n describes the sharpness of the resistive transition. A reasonable value for n in Nb-Ti-copper composites [10] is $n = 50$, which is the value chosen in this study. In practice however, n decreases with b and T [11]. The CSM is retrieved in the asymptotic regime ($n \to \infty$) of Eq. (5).

To solve the magnetic system of equations, the magnetic field h-ϕ formulation is chosen as it has proven to be the most stable and efficient in dealing with the strong non-linearity of the power law [3]. At any instant, the hysteresis power loss per unit volume $q_{\mathrm{hys},1}$ is evaluated as

$$q_{\mathrm{hys},1} = \frac{4}{\pi d_f^2} \int_0^{d_f/2} \int_0^{2\pi} j \cdot e\, r\, dr d\theta. \tag{6}$$

As a boundary condition, the uniform external flux density b_a is applied on the outer boundary of the domain. In this section, it varies from 0 to $b_{a,\max} = 2$ T with a constant ramp rate $\dot{b}_a$. The ramp rate is varied in the study.

Constant Critical Current Density First, to satisfy Carr's assumptions, the critical current density is assumed constant, here $j_c = 5\ 10^9$ A/m^2. In this part, no transport current is imposed in the filament.

The impact of the ramp rate $\dot{b}_a$ on hysteresis losses computed numerically is represented in Fig. 2. As can be observed, Eq. (3) is consistent with the results at very low fields, while Eq. (4) is accurate for $b_a < 0.04$ T. Even though it provides one single approximation for the whole field range, Eq. (4) underestimates the losses in the intermediate regime. In particular, Eq. (2) is almost satisfied as soon as the filament is fully penetrated and it should be preferred over Eq. (4) in the $b_a > b_p$ range.

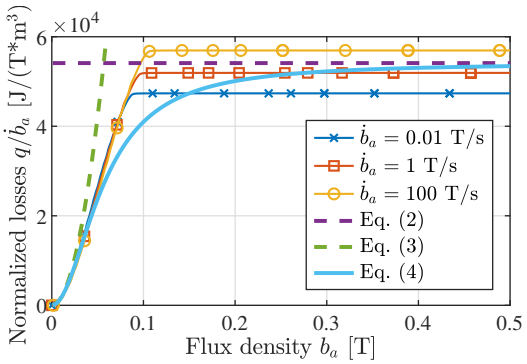

Figure 2: Hysteresis losses $q_{\mathrm{hys},1}$ per unit volume (Eq. (6)) for a monotonic applied field ramp-up at various rates $\dot{b}_a$. For clarity, losses are normalized by the ramp rate $\dot{b}_a$. Results obtained with $n = 50$ and constant $j_c = 5e9$ A/m^2 corresponding to an expected $b_p = 0.102$ T.

As opposed to the CSM and Eq. (2), the $q_{\mathrm{hys},1}/\dot{b}_a$ ratio in full penetration increases with the ramp rate. In a fully penetrated filament subjected to a constant $\dot{b}_a$ along the y-axis, the induced electric field along the filament axis is $e_z \approx x\dot{b}_a$. From Eq. (5) and the analytical evaluation of Eq. (6), the losses per unit volume are given by:

$$q_{\mathrm{hys},1} = \frac{\int_{-\pi/2}^{\pi/2} (cos\theta)^{(n+1)/n}\, d\theta}{(3 + 1/n)\, \pi} j_c d_f \dot{b}_a \left(\frac{d_f \dot{b}_a}{2 e_c} \right)^{1/n}, \tag{7}$$

which tends towards Eq. (2) in the asymptotic regime. The maximal relative error between Eq. (7) and the numerical results is 0.13% for the different ramp rates investigated in Fig. 2, which highlights its accuracy.

Full penetration occurs sooner as the ramp rate is decreased. By analogy between Eq. (2) and Eq. (7), an estimation of the effective penetration flux density b_p^* can be obtained by multiplying Eq. (7) by $3\mu_0/2\dot{b}_a$. Moreover, the evolution of the losses before penetration can be tabulated or fitted as a polynomial function of b_a/b_p^*.

ISBN: 978-3-95450-231-8 ISSN: 2673-5490 doi: 10.18429/JACoW-IPAC2023-THPM095

Critical Current Dependence on Flux Density In practice, the critical current density decreases as the applied magnetic field increases. It can be represented by Kim's [8] model. In this work, Bottura's relationship [12] is preferred as it is consistent both with low field magnetization and high field transport current measurements [13]. In the code, the fitting parameters are those obtained by Bottura with the Spencer [14] data set and $j_c(5\ \mathrm{T}, 4.2\ \mathrm{K}) = 2783\ \mathrm{A/mm^2}$. Figure 3 represents the impact of the ramp rate on the normalized hysteresis losses in the case of the non-linear $j_c(b)$ relation. Both asymptotic regimes are accurately described by Eq. (2) and Eq. (3), even though the equations were established assuming $\partial j_c/\partial b = 0$. However, in the intermediate regime, the losses are greater than the prediction of Eq.(4) and Eq. (2). The filament behaviour is more complex and the determination of b_p^* is not obvious.

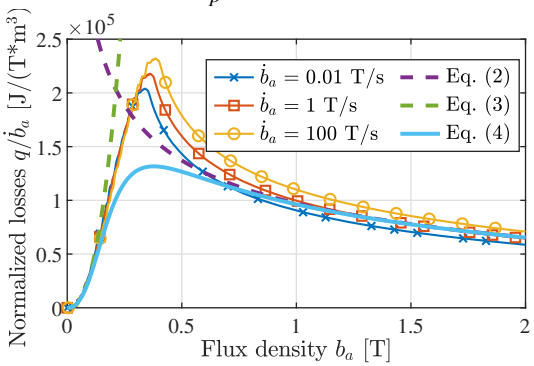

Figure 3: Hysteresis losses $q_{\mathrm{hys},1}$ per unit volume (Eq. (6)) for a monotonic field ramp-up at various $\dot{b}_a$. Results obtained with $n = 50$ and Bottura's $j_c(b)$ relationship [12].

Impact of Transport Current In this section, the critical current density is assumed constant with $j_c = 5\ 10^9\ \mathrm{A/m^2}$ and the transport current ratio $i = I_t/I_c = I_t/(\pi d_f^2 j_c/4)$ [-] is introduced. Numerically, the transport current I_t is established in the system (linear increase during 2 s, stand-by for 1 s) before the external field is increased linearly from 0 to 2 T in 2 s. Its impact is represented in Fig. 4.

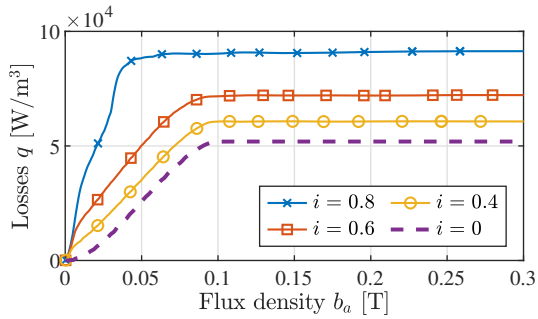

Figure 4: Hysteresis losses $q_{\mathrm{hys},1}$ per unit volume (Eq. (6)) for a monotonic applied field ramp-up at rate $\dot{b}_a = 1\ \mathrm{T/s}$. Results obtained with $n = 50$ and constant $j_c = 5e9\ \mathrm{A/m^2}$ corresponding to an expected $b_p = 0.102\ \mathrm{T}$.

In the fully penetrated regime $b_a > b_p$, the relative increase of losses of $(1+i^2)$ predicted by Wilson [6] for a cyclic transverse field is observed but the relative error increases with i (from 0.7 % at $i = 0.4$ to 7 % at $i = 0.8$). Carr [4] proposed a similar but more complex relation. Before penetration, the relative increase of losses is more significant and more complex to predict analytically. Moreover, the penetration flux density is decreased as i is increased.

LOSSES DURING RAMP-UP

The C400 cyclotron is energized from zero to nominal current in 2 hours. Numerically, the coil cross-section is subdivided in 48 zones. In each zone, the mean flux density and the mean filament current evolution are retrieved from a macroscopic magnetodynamic resolution. Based on these inputs, the hysteresis losses are computed using the single filament model. The integrated losses are represented in Fig. 5 and are compared to the estimate of Eq. (4), which again underestimates losses in the first part of the curve. However, in the second part of the ramp-up, Eq. (4) overestimates the losses, which could be partly explained by the impact of the ramp rate (Eq. (7)) and the long ramp-up time leading to a small $\dot{b}_a$. Inter-filament coupling losses, based on Eq. (1), are negligible as their maximal instantaneous value is 3.6 mW at $t = 800$ s. For computational efficiency reasons, the transient simulation has been performed in a 2D axisymmetric configuration, neglecting the valleys of the yoke and the extraction channels.

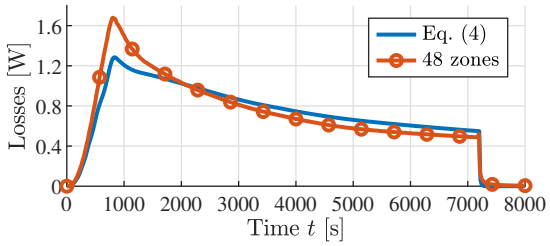

Figure 5: Integrated hysteresis losses Q_{hys} [W] assuming a linear current ramp-up of 7200 s.

CONCLUSION

In this study, different analytical approximations for losses in superconductors have been analyzed. When compared to a finite-element model at the filament scale based on the power law, they have proven to be accurate in full penetration. Numerical results also highlighted the complex behaviour in low field and the significant impact of transport current.

The single filament model allowed the calculation of hysteresis losses during energization of the C400 using a multi-scale approach, taking into account a larger number of parameters and increasing the accuracy of the results. The impact of coupling losses between filaments was shown to be negligible. The model developed in this study provides a flexible tool for estimating AC losses in the coil for different current ramp-up scenarios. As a result, the ramp-up shape can be optimized to minimize the heat load.

As shown in this work, losses in superconductors depend on many physical quantities. Next, the temperature dependence should be introduced at the microscopic scale and coupling losses between twisted filaments should be studied on the basis of a similar analysis.

ISBN: 978-3-95450-231-8 ISSN: 2673-5490 doi: 10.18429/JACoW-IPAC2023-THPM095

REFERENCES

[1] P. Dular, C. Geuzaine, F. Henrotte, and W. Legros, "A general environment for the treatment of discrete problems and its application to the finite element method", *IEEE Trans. Magn.*, vol. 34, no. 5, pp. 3395-3398, Sept. 1998. doi: 10.1109/20.717799.

[2] J. Mandrillon *et al.*, "Status on NHa C400 cyclotron for hadrontherapy", presented at CYC2022, Beijing, China, Dec. 2022, paper THBI01.

[3] J. Dular, "Standard and Mixed Finite Element Formulations for Systems with Type-II Superconductors", Ph.D. thesis, Faculty of Applied Sciences, University of Liège, Liège, Belgium, 2023.

[4] W. J. Carr Jr., *AC loss and macroscopic theory of superconductors*. 2nd edition, Ed. London: Taylor and Francis, 2001. doi:10.1201/9781482264760.

[5] N. J. Simon, E. S. Drexler, and R. P. Reed, "Properties of copper and copper alloys at cryogenic temperatures. Final report.", United States: *NIST publication*, 1992. doi:10.2172/5340308.

[6] M. N. Wilson, *Superconducting magnets*. Oxford University Press, 1983.

[7] C. Bean, "Magnetization of hard superconductors", *Phy. Rev. Lett.*, vol. 8, no. 6, p. 250, March 1962. doi:10.1103/PhysRevLett.8.250.

[8] Y.B. Kim, C.F. Hempstead, and A.R. Strnad, "Critical persistent currents in hard superconductors", *Phy. Rev. Lett.*, vol. 9, pp. 306-309, Oct. 1962. doi:10.1103/PhysRevLett.9.306.

[9] P. W. Anderson, "Theory of flux creep in hard superconductors", *Phy. Rev. Lett.*, vol. 9, p. 309, Oct. 1962. doi:10.1103/PhysRevLett.9.309.

[10] A. K. Ghosh, "V–I transition and n-value of multifilamentary LTS and HTS wires and cables", *Physica C: Superconductivity*, vol. 401, issues 1–4, pp. 15-21, 2004. doi:10.1016/j.physc.2003.09.006.

[11] A. Godeke *et al.*, "Interlaboratory comparisons of Nb-Ti critical current measurements", *IEEE Trans. Appl. Supercond.*, vol. 19, no. 3, pp. 2633-2636, June 2009. doi:10.1109/TASC.2009.2019096.

[12] L. Bottura, "A practical fit for the critical surface of Nb-Ti", *IEEE Trans. Appl. Supercond.*, vol. 10, no. 1, pp. 1054-1057, March 2000. doi: 10.1109/77.828413.

[13] T. Boutboul, S. Le Naour, D. Leroy, L. Oberli, and V. Previtali, "Critical current density in superconducting Nb-Ti strands in the 100 mT to 11 T applied field range", *IEEE Trans. Appl. Supercond.*, vol. 16, no. 2, pp. 1184-1187, June 2006. doi: 10.1109/TASC.2006.870777.

[14] C. Spencer, P. Sanger, and M. Young, "The temperature and magnetic field dependence of superconducting critical current densities of multifilamentary Nb3Sn and Nb-Ti composite wires", *IEEE Trans. Magn.*, vol. 15, no. 1, pp. 76-79, January 1979. doi:10.1109/TMAG.1979.1060146.